



Adsorptive Optimization of Crystal Violet Dye Using Central Composite Rotatable Design and Response Surface Methodology: Statistical Analysis, Kinetic and Isotherm Studies

Thuy Thi Thanh Nguyen¹ · Dong Quy Hoang² · Duyen Thi Cam Nguyen^{3,4} · Thuan Van Tran^{3,4} 

Received: 19 May 2022 / Accepted: 16 October 2022 / Published online: 17 November 2022
© King Fahd University of Petroleum & Minerals 2022

Abstract

Water contamination is emerging as the most critical global issues in the world, calling for the treatment eco-techniques. Taking advantage of biowastes as adsorbent materials is not only in accordance with the purpose of environmental protection but also enhance the higher value-added products. In this work, water hyacinth (*Eichhornia crassipes*) powder was used as an efficient adsorbent for the removal of crystal violet from aqueous solutions. The structure of water hyacinth powder adsorbent was characterized by Fourier transform infrared spectroscopy and scanning electron microscopy analysis. Based on the central composite rotatable design and response surface methodology, the effect of different parameters such as initial pH solution, contact time, adsorbent dosage, and initial crystal violet concentration was optimized. The maximum adsorption capacity of 180.336 mg/g was achieved under the optimum condition as initial pH solution of 6.246, contact time of 125.698 min, the adsorbent dosage of 1.382 g/L, and initial dye concentration of 615.865 mg/L. Moreover, the Langmuir isotherm provided the best fit with a high correlation coefficient of 0.9981 and a maximum monolayer adsorption capacity of 181.818 mg/g at 30 °C. The kinetic studies indicated that the pseudo-second-order model was adequately applied for the adsorption kinetic of crystal violet on the water hyacinth powder adsorbent. The utilization of the water hyacinth plant, an abundant species, as a low-cost biosorbent to remove crystal violet using the central composite rotatable design combined with response surface methodology approach is recommended for the real treatment of organic dyes.

Keywords Water hyacinth · Dye pollution · Crystal violet · Response surface methodology · Adsorption modeling

1 Introduction

The presence of industrial dyes in wastewater is a very serious environment problem because of their highly toxicity and carcinogenicity. They are known as potential hazards to living organism. Dyes have complex aromatic structures and synthetic origins that make them stable to biodegradation, oxidizing agents, and photodegradation [1]. The undesirability of the presence of dyes in aqueous prevents the passage of light through water, which leads to the reduction of photosynthesis activity and consequently decreases the dissolved oxygen in the water and spoils the ecosystem [1, 2]. Among these dyes, crystal violet (CV), a triphenylmethane dye, is immensely used in the dyeing of textile, the printing of paper, the coloring of leather and paint industry, and then it enters into the aquatic systems that were one of the major causes of water pollution [3]. CV is also well known for its cause of certain serious problems such as mutagenic, teratogenic, and mitotic poisoning nature. A number of

✉ Thuy Thi Thanh Nguyen
nguyenthanhthuy@hcmuaf.edu.vn

✉ Thuan Van Tran
tranvt@ntt.edu.vn; tranuv@gmail.com

¹ Faculty of Science, Nong Lam University, Ho Chi Minh City 700000, Vietnam

² Faculty of Materials Science and Technology, University of Science, Ho Chi Minh City 700000, Vietnam

³ Institute of Applied Technology and Sustainable Development, Nguyen Tat Thanh University, 298-300A Nguyen Tat Thanh, District 4, Ho Chi Minh City 755414, Vietnam

⁴ NTT Hi-Tech Institute, Nguyen Tat Thanh University, 298-300A Nguyen Tat Thanh, District 4, Ho Chi Minh City 755414, Vietnam



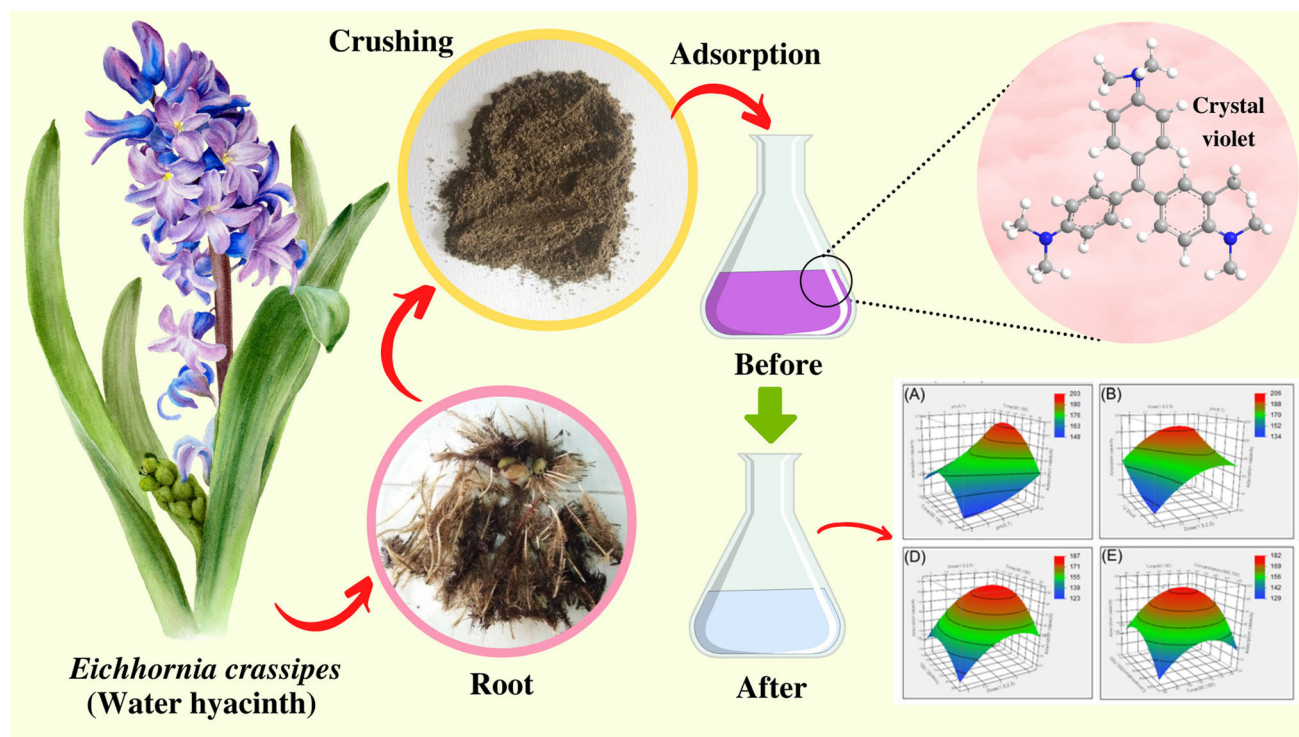


Fig. 1 Illustrative preparation and crystal violet adsorption performance of biosorbent powder derived from water hyacinth species

Table 1 Coded units used for the variable parameters for the statistical analysis

Variable	Unit	Coded values				
		$-\alpha$	-1	0	$+1$	$+\alpha$
pH solution (X_1)		4	5	6	7	8
Contact time (X_2)	min	60	90	120	150	180
Adsorption dosage (X_3)	g/L	1	1.5	2	2.5	3
Initial concentration of CV (X_4)	mg/L	400	500	600	700	800

methods aimed at removing CV from the wastewaters have been studied such as coagulation, adsorption, flocculation, reverse osmosis, biological methods, and membrane filtration [4]. Amid them, adsorption is one of the most effective techniques thanks to its advantages such as great ease of operation, selectivity, sensitivity, low cost, and low energetic requirements [5]. Nowadays, many kinds of composites and advanced materials have been developed for adsorption and adsorption integrated degradation of hazardous contaminants including CV in water [6, 7]. However, their disadvantages can be multi-step synthesis procedure, using toxic chemicals for material production, and eco-unfriendliness. Therefore, utilization of green and sustainable adsorbents is highly expected in the field.

The use of biomass as an adsorbent has been gained much attention. Indeed, many publications have revealed the use of various biomass adsorbents for the efficiency treatment of

dyes from textile wastewaters such as rice husk ash [8], grapefruit peel [9], ginger waste [10], tomato plant root [11], date palm fiber [12], teak leaf powder [12], and waste black tea [13]. Considering advantages of these adsorbents, they are mainly derived from eco-friendly, low-cost, safe, and sustainable biowastes or agricultural by-products. As a result, the conversion of these biowastes into effective adsorbents is not only in accordance with the purpose of alleviating environmental pollution but also promotes the value of wastes for value-added products.

Water hyacinth (*Eichhornia crassipes*) is an aquatic weed plant and one of the most typical invasive species. They can be found ubiquitously in rivers, lakes, ponds, canals, and agricultural fields. Because of their very strong adaptability, reproduction, and spreading powers, water hyacinth has posed an alarming threat to indigenous plants, water quality, soil, as well as biodiversity [14]. To mitigate the harmful

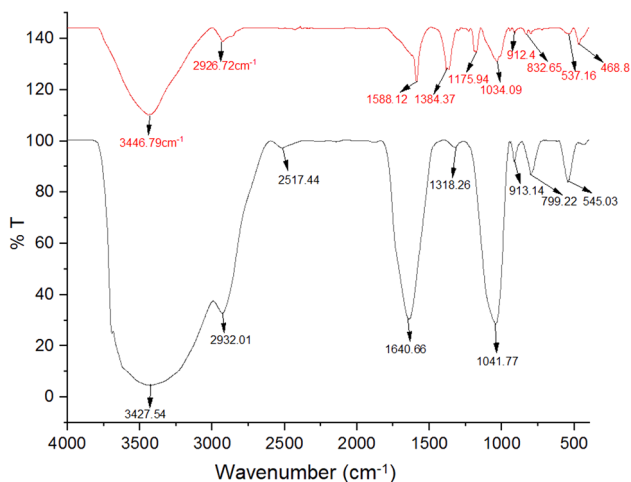


Fig. 2 FTIR spectra of WHP before adsorption (red line) and after adsorption (black line) of CV dye

Table 2 Biosorption equilibrium and kinetic models

Models		Nonlinear equation
Nonlinear isotherm model	Langmuir	$q_e = \frac{Q_0 K_L C_e}{1 + K_L C_e}$
	Freundlich	$\log q_e = \log K_F + \frac{1}{n} \log C_e$
Kinetic model	Pseudo-first order	$\log(q_e - q_t) = \log q_e - \frac{K_1}{2.303} t$
	Pseudo-second order	$\frac{t}{q_t} = \frac{1}{K_2 q_e^2} + \frac{1}{q_e} t$

effect of this species, a new protocol of transforming water hyacinth into biosorbents is worth considered. Indeed, water hyacinth can be used as a bioadsorbent to adsorb various industrial dyes such as CV, methylene blue, Congo red, and Vitoria blue from aqueous media [15]. Some parts of

water hyacinth plant such as roots and leaves can be used as effective materials for removing dyes from the industrial wastewaters. A number of publications investigated the use of the water hyacinth-based biosorbents, biocomposites, and bio-based photocatalysts to improve the dye removal efficiency [16–18]. However, the production of these adsorbents often prolonged and required toxic chemicals, leading to the possibility of secondary pollution. Moreover, the adsorption data in these works were analyzed in the form of univariate, which can lead to statistical mistakes and misunderstanding of synergistic interactions among adsorption parameters (e.g., concentration, dosage, pH, time, temperature, etc.). Difference from multivariate experiments and univariate experiments endures step-by-step investigations, resulting in the fact that a large number of trials is required. In many cases, optimum values rely completely on the results of all trials. As such, it is important to develop optimization approaches to aid the treatment process efficiently and reduce the number of trials.

Response surface methodology (RSM) is considered a common and easy-to-use tool to predict the processes in chemistry in order to reduce the number of experimental runs and produce high-quality products [19]. RSM describes the relationship between several independent variables and various dependent variables [20]. For instance, Eddebbagh et al. [21] reported a procedure based on the central composite design combined with response surface methodology to optimize the conditions of several parameters such as the activation temperature, activation time, and chemical impregnation. They found that the removal of methylene blue at optimized process conditions was 90.5%. In a previous study conducted by Moughaoui et al. [22], the optimum adsorption of methylene blue and malachite green was investigated with sugarcane bagasse adsorbent using RSM. Their work showed a good correlation between the predicted factors of the RSM model and the obtained experimental values. Therefore, the central composite rotatable design combined with response

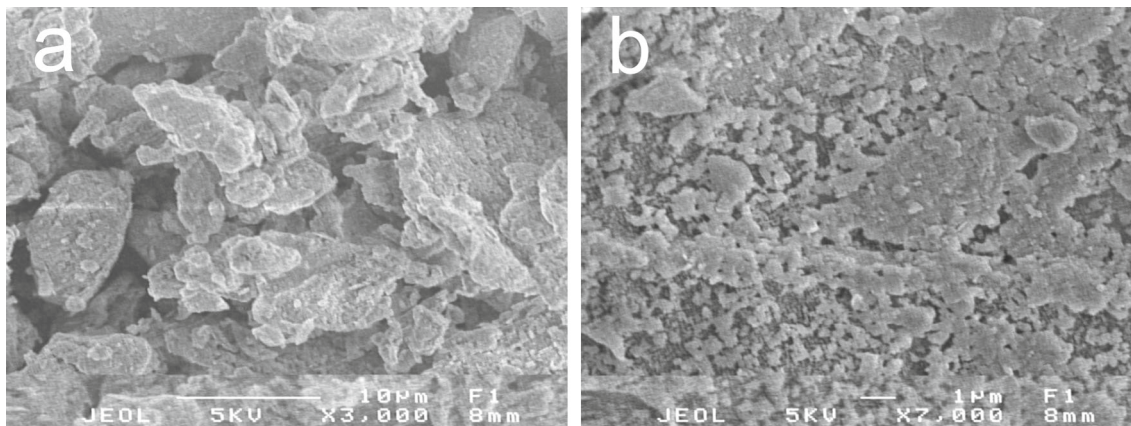


Fig. 3 SEM images of WHP before (a) and after (b) adsorption of CV dye

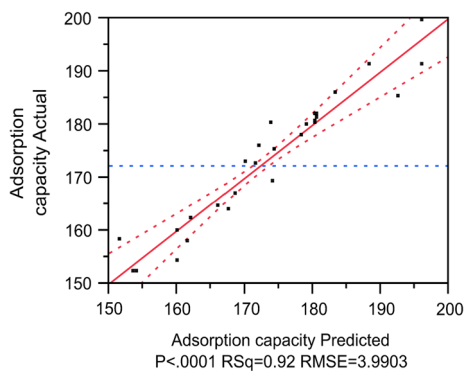


Fig. 4 Actual and predicted plot of CV adsorption capacity (q_e)

surface methodology can be a useful tool for optimization of dyes removal from wastewaters.

The objectives of this research, therefore, involve (i) to apply central composite rotatable design (CCRD) combined with RSM in order to get the convenient adsorption conditions and optimization modeling for the maximizing adsorption capacity of water hyacinth powder (WHP) for CV removal from aqueous solution; (ii) to understand the effects of four independent variables such as the initial pH solution, the contact time, the adsorbent dosage, and the initial concentration of CV and their interactions on the adsorption capacity of WHP for CV; (iii) to study the adsorption isotherms and kinetic models of CV adsorption on WHP.

2 Materials and Methods

2.1 Materials

Crystal violet ($C_{25}H_{30}N_3Cl$, Sigma – USA), sodium hydroxide (NaOH, Merck-Germany), and hydrochloric acid (HCl, Xilong Scientific Co., Ltd, China) were used without further purification. Stock solution (1000 mg/L) was prepared by dissolving accurately the weight quantity of the CV (1.0 g) in distilled water. Experimental CV solutions of different concentrations were prepared by the dilution of a stock solution. The initial solution pH was adjusted with HCl 0.1 M and NaOH 0.1 M solution.

2.2 Preparation of Biosorbent

Water hyacinth plants, which were used in this study, were collected from Saigon River, Ho Chi Minh City, Vietnam. The water hyacinth was washed with distilled water to remove dust and dried at 60 °C for 24 h. After, the dried plants were sieved with particle size lower than 0.15 mm and stored in a desiccator until used.

2.3 Biosorption Studies

WHP biosorption studies (Fig. 1) were performed in batch using the colored solution of CV, wherein dye volume and the stirring speed were maintained at 25 mL and at 500 rpm, respectively, in all the experimental runs. In this experiment, the effect of variables such as the initial pH solution (2–9), the contact time (10–240 min), the adsorbent dosage (0.1–3.0 g), and the initial concentration of CV (100–600 mg/L) was studied. The amount of dye adsorbed by the biosorbent and the percent removal dye from the solution were determined based on the difference between the initial dye concentration and the dye concentration in the following Eqs. 1 and 2:

$$q = \frac{(C_0 - C) \times V}{m} \quad (1)$$

$$\% \text{ removal} = \frac{(C_0 - C)}{C_0} \times 100 \quad (2)$$

where q is the amount of dye taken up by the biosorbent (mg/g), C_0 is the initial concentration of dye (mg/L), C is the concentration of dye in the supernatant (mg/L), V is the volume of the solution (L), and m is the mass of biosorbent (g).

2.4 Experimental Design

The estimation of the optimum conditions of CV removal from aqueous solution using WHP adsorbent depends on the factors such as the initial pH solution, the contact time, the adsorbent dosage, and the initial dye concentration. RSM and CCRD were used to investigate the effects of the four independent variables on response surface for optimization of adsorption conditions [23]. In this work, a total of 52 experiments were employed to evaluate the individual and interactive effects of the four main independent parameters on the CV adsorption efficiency. The maximizing adsorption capacity of WHP for CV removal from aqueous solution was carried out as a response Y of the system under four process parameters, namely the initial pH solution: 2–8, the contact time: 60–180 min, the adsorbent dosage: 1–3 g/L, the initial concentration of CV: 400–800 mg/L. The variables and levels of the design model are given in Table 1. Using this design, the experimental data were fitted according to Eq. 3 as a quadratic polynomial equation including individual and cross-effects of variables.

$$Y = \beta_0 + \beta_1 X_1 + \beta_2 X_1^2 + \beta_3 X_2 + \beta_4 X_2^2 + \beta_5 X_3 + \beta_6 X_3^2 + \beta_7 X_4 + \beta_8 X_4^2 + \beta_9 X_1 X_2 + \beta_{10} X_1 X_3 + \beta_{11} X_1 X_4 + \beta_{12} X_2 X_3 + \beta_{13} X_2 X_4 + \beta_{14} X_3 X_4 \quad (3)$$

where $\beta_0, \beta_1, \beta_2, \dots, \beta_{14}$ are regression coefficients, Y is the maximizing adsorption capacity (response), X_1 is the initial pH solution, X_2 is the contact time, X_3 is the adsorbent dose, and X_4 is the initial concentration of CV. Multiple regression analysis, response surface plots, and statistical analyses were performed using JMP 10 software (SAS Institute, North Carolina, USA).

2.5 Equilibrium and Kinetic Models

In this study, the classical models of Langmuir and Freundlich were used in order to describe the equilibrium between biosorption capacity and sorbate concentration at a constant temperature. The nonlinear pseudo-first-order and pseudo-second-order models were applied to study the adsorption kinetic [24]. The equations are presented in Table 2. where q_e is the equilibrium dye uptake per g of the biosorbent (mg/g), q_t is the amount of dye adsorbed at time t (mg/g), K_L is the Langmuir constant (L/mg), K_F is the Freundlich constant (mg/g), n is a constant dependent on the nature of adsorbate and temperature, and Q_0 is the adsorption capacity (mol/L).

3 Results and Discussion

3.1 Characterization of Water Hyacinth Powder

The FTIR spectrum of WHP before (red line) and after (black line) adsorption of CV was shown in Fig. 2. The presence of a peak at 3427 cm^{-1} indicates the O – H stretching. The peak at 2932 cm^{-1} can be ascribed to the stretching vibration of the C – H bonds. The peaks were observed at 1640 cm^{-1} , 1318 cm^{-1} , and 1041 cm^{-1} , which were associated with C = O, C – O, and sulfonic groups, respectively. After biosorption, the appearance of a peak at 1588 cm^{-1} reflected the C-N group, and the disappearance of the peak at 1318 cm^{-1} corresponded to the –CO group. Furthermore, the characteristic –OH band at 3427 cm^{-1} shifted to 3446 cm^{-1} confirmed the participation of these groups in the dye uptake. Similar results were also reported by Kumar et al. [10] and Saha et al. [25]. The results of functional groups on water hyacinth powder by FTIR analysis as a main characterization in this work were also in accordance with the previous work [26, 27].

The textual structure examination of WHP particles can be observed before and after the biosorption of CV from the SEM (Fig. 3). Before dye uptake, the PR-WH particles show porous and irregular surfaces (Fig. 3a). The pores were partially filled after the adsorption of CV, showing the CV adsorbed on the surface of WHP (Fig. 3b). This finding indicates that the adsorption of CV molecules over WHP occurred.

3.2 Response Surface Methodology

The influence of experimental conditions with four variable parameters, namely the initial pH solution, the contact time (min), the adsorbent dosage (mg/g), and the initial concentration of CV (mg/L) on the CV adsorption, was studied using RSM. The total of 52 experiments is shown in Table 3. The relationship between variables and response can be represented in Eq. 4.

$$Y(q_e) = 180.33588 + 6.1529438 X_1 + 3.4459979 X_2 - 7.319777 X_3 + 3.5297188 X_4 + 2.1051781 X_3 X_4 - 3.375615 X_2^2 - 2.900884 X_3^2 - 3.298121 X_4^2 \quad (4)$$

The diagnostic plot of the model is shown in Fig. 4. Accordingly, the coefficient of linear regression R^2 of 0.92, which is higher than 0.80, indicating the fitness of polynomial models used for describing the effect of variables on the response would be more accurate and 8% of the variations are not considered [28–30]. The results indicated that there was an agreement between the experimental and the prediction in adsorption capacity of WHP.

The analysis of variance (ANOVA) for the response surface quadratic model is given in Table 4. The ANOVA results indicated that a model with a large F -value of 30.6818 and p -value < 0.0001 is more significant. When the p -value < 0.01 is typically viewed as an indication, the model was adequate to explain the correlation between the factors and the corresponding response [31]. The lack of fit was significant with a F -value of 44.1986 and a p -value < 0.0001 . The probability of F -values which are fewer than 0.05 indicated that the model terms are significant [32]. It is obvious that the p -value is found to be less than 0.005 for all four individual parameters such as the initial pH solution (X_1), the contact time (X_2), the adsorbent dosage (X_3), and the initial concentration of CV (X_4) under linear conditions (Table 5). The model contained a six two-way interaction (the initial pH solution x the contact time, the initial pH solution x the adsorbent dosage, the contact time x the adsorbent dosage, the initial pH solution x the initial concentration of CV, the contact time x the initial concentration of CV, and the adsorbent dosage x the initial concentration of CV). Only the cross-interaction between the adsorbent dosage and the initial dye concentration was significant while all the rest of these interactions did not have a significant effect on the determination of the CV adsorption since the p -value was more than 0.05. However, the quadratic effects of X_2^2 , X_3^2 , and X_4^2 were all signed with a p -value < 0.001 showing that the variables had a great influence on the CV adsorption capacity of the WHP. The 3-D response surface plots used for the predicted responses are shown in Fig. 5 that confirming the presence of strong interaction between

Table 3 The observed (Y) and the predicted values of the response

Run no	Uncoded values				Coded values				q _e (mg/g)	
	X ₁	X ₂	X ₃	X ₄	X ₁	X ₂	X ₃	X ₄	Observed values (Y)	Predicted values
1	6	120	2.0	600	0	0	0	0	180.446	180.502
2	5	90	1.5	500	-1	-1	-1	-1	166.855	168.783
3	7	90	1.5	500	+1	-1	-1	-1	179.891	179.258
4	5	150	1.5	500	-1	+1	-1	-1	169.303	174.255
5	7	150	1.5	500	+1	+1	-1	-1	191.400	188.361
6	5	90	2.5	500	-1	-1	+1	-1	158.227	151.758
7	7	90	2.5	500	+1	-1	+1	-1	162.345	162.244
8	5	150	2.5	500	-1	+1	+1	-1	152.231	153.569
9	7	150	2.5	500	+1	+1	+1	-1	163.912	167.687
10	5	90	1.5	700	-1	-1	-1	+1	172.923	179.188
11	7	90	1.5	700	+1	-1	-1	+1	181.837	180.682
12	5	150	1.5	700	-1	+1	-1	+1	178.071	178.529
13	7	150	1.5	700	+1	+1	-1	+1	185.185	192.654
14	5	90	2.5	700	-1	-1	+1	+1	158.067	161.583
15	7	90	2.5	700	+1	-1	+1	+1	175.970	172.088
16	5	150	2.5	700	-1	+1	+1	+1	164.670	166.264
17	7	150	2.5	700	+1	+1	+1	+1	181.996	180.401
18	4	120	2.0	600	- α	0	0	0	172.693	171.564
19	8	120	2.0	600	+ α	0	0	0	199.592	196.176
20	6	60	2.0	600	0	- α	0	0	154.269	160.107
21	6	180	2.0	600	0	+ α	0	0	180.226	173.891
22	6	120	1.0	600	0	0	- α	0	186.127	183.538
23	6	120	3.0	600	0	0	+ α	0	152.103	154.259
24	6	120	2.0	400	0	0	0	- α	159.911	160.250
25	6	120	2.0	800	0	0	0	+ α	175.079	174.369
26	6	120	2.0	600	0	0	0	0	180.132	180.502
27	6	120	2.0	600	0	0	0	0	180.540	180.170
28	5	90	1.5	500	-1	-1	-1	-1	166.792	168.452
29	7	90	1.5	500	+1	-1	-1	-1	179.975	178.927
30	5	150	1.5	500	-1	+1	-1	-1	169.429	173.923
31	7	150	1.5	500	+1	+1	-1	-1	191.400	188.030
32	5	90	2.5	500	-1	-1	+1	-1	158.187	151.426
33	7	90	2.5	500	+1	-1	+1	-1	162.305	161.912
34	5	150	2.5	500	-1	+1	+1	-1	152.261	153.238
35	7	150	2.5	500	+1	+1	+1	-1	163.952	167.355
36	5	90	1.5	700	-1	-1	-1	+1	173.049	169.857
37	7	90	1.5	700	+1	-1	-1	+1	181.293	180.351
38	5	150	1.5	700	-1	+1	-1	+1	177.945	178.198
39	7	150	1.5	700	+1	+1	-1	+1	185.311	192.323
40	5	90	2.5	700	-1	-1	+1	+1	158.142	161.252
41	7	90	2.5	700	+1	-1	+1	+1	176.070	171.757
42	5	150	2.5	700	-1	+1	+1	+1	164.595	165.933

Table 3 (continued)

Run no	Uncoded values				Coded values				q _e (mg/g)	
	X ₁	X ₂	X ₃	X ₄	X ₁	X ₂	X ₃	X ₄	Observed values (Y)	Predicted values
43	7	150	2.5	700	+ 1	+ 1	+ 1	+ 1	181.846	180.070
44	4	120	2.0	600	− α	0	0	0	172.599	171.232
45	8	120	2.0	600	+ α	0	0	0	191.400	195.844
46	6	60	2.0	600	0	− α	0	0	154.175	159.776
47	6	180	2.0	600	0	+ α	0	0	180.132	173.560
48	6	120	1.0	600	0	0	− α	0	185.939	183.206
49	6	120	3.0	600	0	0	+ α	0	152.229	153.927
50	6	120	2.0	400	0	0	0	− α	159.879	159.918
51	6	120	2.0	800	0	0	0	+ α	175.173	174.037
52	6	120	2.0	600	0	0	0	0	180.226	180.170

Table 4 Analysis of variances for optimization of CV adsorption capacity (q_e) using the JMP software

Source	DF	Adj. SS	Adj. MS	F-value	p-value
Model	14	6839.3151	488.523	30.6818	< 0.0001
Residuals (error)	37	589.1225	15.922		
Lack of fit	10	555.20613	55.5206	44.1986	< 0.0001
Pure error	27	33.91638	1.2562		
Total	51	7428.4376			
			R ²	0.920694	
			Adjusted R ²	0.890686	

DF Degree of freedom; SS Sum of square; MS Mean square

Table 5 Estimated regression coefficients and their significance

Source	Estimate	Std. error	t-value	p-value	Remark
Intercept	180.33588	1.995133	90.39	< 0.0001	Significant
X ₁	6.1529438	0.575945	10.68	< 0.0001	Significant
X ₂	3.4459979	0.575945	5.98	< 0.0001	Significant
X ₃	− 7.319777	0.575945	− 12.71	< 0.0001	Significant
X ₄	3.5297188	0.575945	6.13	< 0.0001	Significant
X ₁ *X ₂	0.9078531	0.705386	1.29	0.2061	
X ₁ *X ₃	0.0028469	0.705386	0.00	0.9968	
X ₂ *X ₃	− 0.914922	0.705386	− 1.30	0.2026	
X ₁ *X ₄	0.0047281	0.705386	0.01	0.9947	
X ₂ *X ₄	0.7174344	0.705386	1.02	0.3157	
X ₃ *X ₄	2.1051781	0.705386	2.98	0.0050	Significant
X ₁ ²	0.8420599	0.675356	1.25	0.2203	
X ₂ ²	− 3.375615	0.675356	− 5.00	< 0.0001	Significant
X ₃ ³	− 2.900884	0.675356	− 4.30	0.0001	Significant
X ₄ ⁴	− 3.298121	0.675356	− 4.88	< 0.0001	Significant

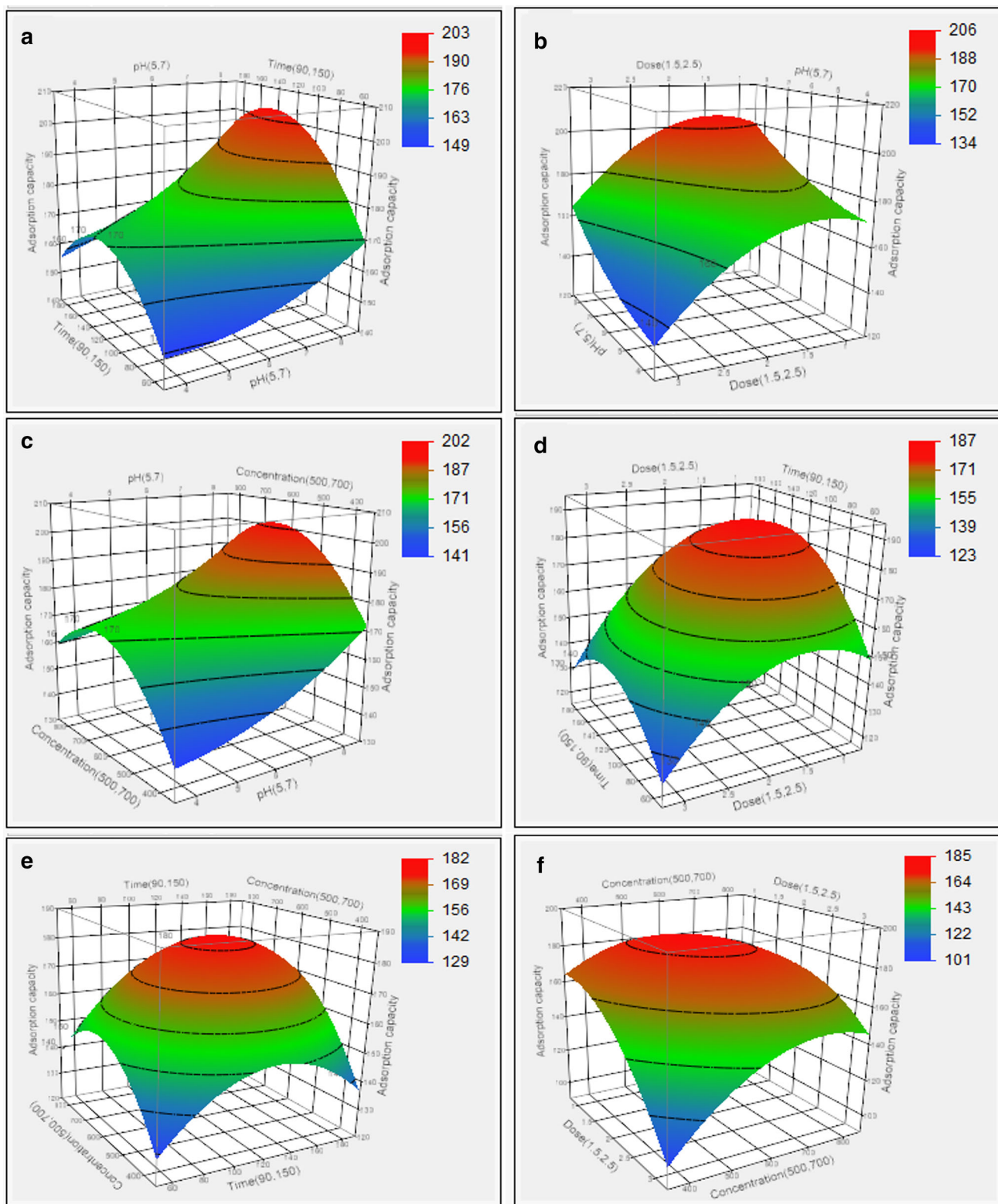


Fig. 5 The 3D plots showing the effect of **a** the initial pH solution and the contact time, **b** the initial pH solution and the adsorbent dosage, **c** the initial pH solution and the initial dye concentration, **d** the contact

time and the adsorbent dosage, **e** the contact time and the initial dye concentration, **f** the adsorbent dosage and the initial dye concentration on the CV adsorption capacity

each pair variable. The interaction of the initial pH solution with the contact time, the adsorbent dosage, and the initial CV concentration on the CV adsorption capacity response is shown in Figs. 4a, b, and c. The results indicated that the CV adsorption capacity of the WHP increased with increasing pH from 4 to 6 and slightly increased from pH 6 to 8. It seems that the maximum adsorption was found to be at pH 6. This result could be explained as due to the electrostatic repulsion interaction between the negatively charged WHP particles and the positively charged dye molecule [33]. Thus, as the H^+ ions concentration in the solution decreased, the numbers of negative charges increased which results in an increase in the percentage removal of CV. Similar observations have been reported by Saeed et al. [9].

The effect of the contact time with the initial pH solution, the adsorbent dosage, and the initial CV concentration are visualized in Figs. 5a, d, and e. From these data, it is revealed that the dye CV was rapidly adsorbed at the beginning of the experiment until 120 min due to a large number of vacant sites on the adsorbent particles surface available for the adsorption of CV and then relatively stable from 120 to 150 min. The interaction of the adsorbent dosage with other independent process variables is presented in Figs. 5b, d, and f. It can be observed that the adsorption efficiency increased with the increase in the adsorbent dosage from 1 to 2 g/L and then remained almost constant with a further increase in the adsorbent dosage. These results could be due to the increase in available surface area and consequently more active sites for efficient adsorption [34].

The optimum conditions for the initial pH solution, the contact time, the adsorbent dosage, and the initial concentration of CV were found to be 6.246, 125.698 min, 1.382 g/L, and 615.865 mg/L, respectively. At these conditions, the maximum adsorption of the CV dye was 180.336 mg/g with a desirability of 0.600. Under the optimal condition of parameters, the corresponding experimental value of the CV adsorption was 180.071 mg/g, indicating that there was conformity between the experiment results with the optimized values.

3.3 Adsorption Isotherms

In order to investigate the adsorption isotherms of the CV by the water hyacinth powder at different temperatures, two nonlinear isotherm models have been used: Langmuir and Freundlich isotherm models. The isotherm parameters are summarized in Table 6. Data shown in Figs. 5a and b represented the three various equilibrium isotherm models for the adsorption of CV on WHP. By comparing the R^2 obtained from Langmuir and Freundlich isotherms ($R^2 > 0.97$), it can be suggested that the Langmuir isotherm was more favored by the adsorption process at various temperatures. This indicated that the uptakes occur by monolayer adsorption onto a

homogenous surface with a finite number of identical sites. The maximum adsorption capacity q_{max} was 181.818 mg/g, 192.308 mg/g, and 196.078 mg/g at 30 °C, 40 °C, and 50 °C, respectively. According to Table 6, obtained values of separation factor or equilibrium constant R_L were 0.101, 0.111, and 0.105 at 30 °C, 40 °C, and 50 °C, respectively. These findings indicated that the favorability of the adsorption process [35].

To assess the maximum adsorption capacity obtained in this work, a comparison study has been conducted with emphasis on the biosorbents used, adsorption temperature, and capacity. According to Table 7, water hyacinth powder can adsorb crystal violet dye with very high q_m values of 181.18–196.08 mg/g at various temperatures. These outcomes were so far higher than those obtained by *Ficus religiosa* leaves powder and *Daucus carota* pomace powder (2.4–27 mg/g), date palm leaves powder (36.74 mg/g), coffee husks (12.24 mg/g), and anatolian black pine (12.36 mg/g). The water hyacinth powder in this work had higher adsorption performance than modified biosorbents such as charred rice husk (62.85 mg/g) and xanthated rice husk (90 mg/g), but slightly lower than citric acid-modified red seaweed (217.38 mg/g) or centaurea stem powder (476.8 mg/g). The water hyacinth biosorbents also gave good adsorption capacity results in comparison with *Ananas comosus* (pineapple) leaf powder, red seaweed powder, and cottonwood seeds. To sum up, it can be concluded that the water hyacinth powder can be a competitive biosorbent for the removal of crystal violet from water.

3.4 Adsorption Kinetics

In order to study the mechanism of CV adsorption by the WHP at various concentrations of CV, two kinetic models were considered: the pseudo-first-order model proposed by Lagergren and the pseudo-second-order model. Table 8 summarizes the kinetic parameters of the fitted models. Figures 6c and d indicates that the plots of nonlinear pseudo-second-order model showed a higher correlation coefficient R^2 for all initial dye concentrations than that of the pseudo-first-order model. Moreover, the q_e increased with the increase in initial concentration of CV, while the nonlinear pseudo-second-order rate constant K_2 decreased with the increase in initial dye concentration. These results revealed that the pseudo-second-order model is appropriate only to describe the adsorption kinetics of CV by WHP adsorbent and it implies that chemisorption mechanics took place during the adsorption process. This is in accordance with the results obtained by Cheruiyot [49] using coffee husks for the adsorption of toxic crystal violet from an aqueous solution [49].

From the best-fitting results obtained by the pseudo-second-order model, it can be suggested that the adsorption is controlled by chemisorption phenomenon, which surface functional groups are responsible for the interaction with

Table 6 Langmuir and Freundlich constants at different temperatures

Temp. (°C)	Langmuir isotherm				Freundlich isotherm		
	q_{\max} (mg/g)	K_L (L/mg)	R_L (L/mg)	R^2	n	K_F (mg/g)	R^2
30	181.818	0.089	0.101	0.9981	3.836	46.132	0.9709
40	192.308	0.080	0.111	0.9968	3.621	45.352	0.9817
50	196.078	0.085	0.105	0.9967	3.621	46.677	0.9777

Table 7 The comparative adsorption performance of various biosorbents for removal of crystal violet dye

Adsorbents	Adsorption temperature (°C)	q_{\max} (mg/g)	References
Water hyacinth powder	30	181.818	This study
Water hyacinth powder	40	192.308	This study
Water hyacinth powder	50	196.078	This study
<i>Ananas comosus</i> (pineapple) leaf powder	30	158.73	[36]
<i>Ananas comosus</i> (pineapple) leaf powder	20	78.22	[37]
Artocarpus altilis (Breadfruit) skin powder	25	145.8	[38]
<i>Cordia trichotoma</i> sawdust	55	129.77	[39]
Lemongrass leaf fibers	25	36.1	[40]
Date palm leaves powder	56	37.736	[41]
Red seaweed powder	20	142.86	[42]
Citric acid-modified red seaweed	20	217.38	[42]
Apple stem powder	35	153.85	[43]
<i>Cucumis Sativus</i> peel powder	25	149.25	[44]
<i>Ficus religiosa</i> leaves powder	70	2.4	[45]
<i>Daucus carota</i> pomace powder	30	27	[45]
Cottonwood seeds	25	153.85	[46]
Formosa papaya seed powder	25	85.99	[47]
Charred rice husk	25	62.85	[48]
Xanthated rice husk	25	90.02	[48]
Coffee husks	25	12.24	[49]
Anatolian black pine	45	12.36	[50]
Centaurea stem powder	39	476.19	[29]

Table 8 Comparison of kinetic parameters for different initial concentrations CV at 30 °C

C_0 (mg/L)	Pseudo-first order				Pseudo-second order		
	$q_{e(\text{exp})}$ (mg/g)	$q_{e(\text{cal})}$ (mg/g)	k_1 (1/min)	R^2	$q_{e(\text{cal})}$ (mg/g)	k_2 (g/mg min)	R^2
50	48.885	2.600	0.019	0.9098	69.020	0.021	1
100	93.666	7.374	0.019	0.9184	94.340	0.008	1
150	134.887	14.471	0.018	0.8683	131.579	0.004	1

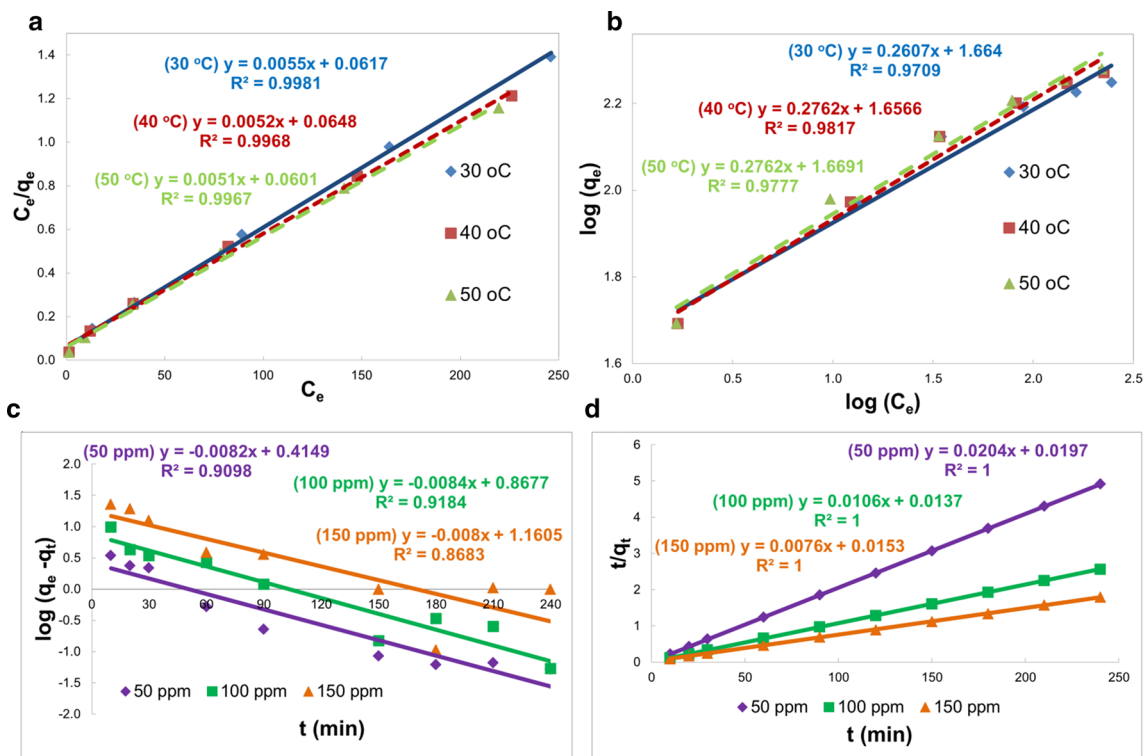


Fig. 6 The adsorption isotherm **a** Langmuir adsorption isotherm and **b** Freundlich adsorption isotherm for the adsorption of CV on water hyacinth powder and the adsorption kinetic, **c** pseudo-first-order plots, and **d** pseudo-second-order plots for the adsorption of CV on WHP

crystal violet molecules. Indeed, the possible interaction between the CV and WHP can be elaborated as follows. WHP adsorbent possess a range of surface functional groups such as hydroxyl and carbonyl groups. These surface functional groups can interact with amine groups of CV through hydrogen interaction. Such interactions have been reported in the previous works, which enhances the adsorption performance of the biomass adsorbent [51]. Moreover, the water hyacinth powder biosorbent was not reusable as it was reflecting the chemical bonding mechanism between the dye molecules and the adsorbent sites. After the adsorption, the loss of surface functional groups led to the significant reduction of reuse performance. As a result, the recycle of water hyacinth powder biosorbent was not successful.

4 Conclusion

In the present work, the water hyacinth powder has been successfully produced via a facile procedure and was found with many surface functional groups. This biosorbent was used as an efficient adsorbent for crystal violet adsorption from the aqueous solution. The central composite rotatable design combined with response surface methodology has been adopted as a powerful tool for optimization of process parameters to maximize the dye adsorption capacity.

It was observed that individual factors such as the initial pH solution, the contact time, the adsorption dosage, and the initial concentration of CV played an important role in the CV adsorption capacity of water hyacinth powder. Under optimum operating points, giving maximum CV adsorption ($q_e = 180.336$ mg/g) was determined as follows: the initial pH solution, 6.246; the contact time, 125.698 min; the adsorbent dosage, 1.382 g/L; and the initial dye concentration, 615.865 mg/L. The tested values were in very high correlation with the predicted model values of the response variable, suggesting high validation and reliability of proposed quadratic model. The adsorption isotherms studies showed that the equilibrium process could be well described by Langmuir model, revealing the monolayer adsorption of dye on water hyacinth powder. The kinetic adsorption also suggested the best fitting of pseudo-second-order kinetic equation, which might confirm the control of surface functional groups toward adsorption process. With high maximum adsorption capacity (181.18–196.08 mg/g) at various temperatures, our findings recommend that water hyacinth powder can be an attractive candidate for removing crystal violet from the wastewater.

Acknowledgements The authors would love to appreciate the effort of researchers all over the world in the fight against the COVID-19 pandemic.

Author Contributions TTTN contributed to conceptualization; methodology; data curation; investigation; validation; writing—original draft. DQH contributed to data curation; methodology; investigation; validation. DTCN contributed to writing—review and editing; validation; English editing; data curation. TVT contributed to conceptualization; writing—review and editing; validation; data curation; supervision; English editing; project administration. All authors read and approved the final manuscript.

Funding There was no external funding for this study.

Data Availability The authors declare that all data and materials support their published claims and comply with field standards.

Code Availability The authors declare that software application or custom code supports their published claims and comply with field standards.

Declarations

Conflicts of interest The authors declare that there are no conflicts of interest.

Ethical Approval All authors have been personally and actively involved in substantive work leading to the manuscript, and will hold themselves jointly and individually responsible for its content.

Consent for Publishing The manuscript has not been published anywhere nor submitted to another journal. The manuscript is not currently being considered for publication in any another journal.

Human and Animal Rights Research does not involve any Human Participants and/or Animals.

References

- Li, F.; He, X.; Srishti, A.; Song, S.; Tan, H.T.W.; Sweeney, D.J.; Ghosh, S.; Wang, C.-H.: Water hyacinth for energy and environmental applications: a review. *Bioresour. Technol.* **327**, 124809 (2021). <https://doi.org/10.1016/j.biortech.2021.124809>
- Estrada-Arriaga, E.B.; García-Sánchez, L.; Falcón-Rojas, A.: Experimental design approach for the removal of the antidiabetic drug, metformin at a high concentration by photocatalytic processes. *Water Environ. J.* **35**, 759–771 (2021). <https://doi.org/10.1111/wej.12668>
- Tran, T.V.; Nguyen, H.-T.T.; Dang, H.H.; Nguyen, D.T.C.; Nguyen, D.H.; Pham, T.V.; Tan, L.V.: Central composite design for optimizing the organic dyes remediation utilizing novel graphene oxide@CoFe₂O₄ nanocomposite. *Surf. Interf.* **21**, 100687 (2020). <https://doi.org/10.1016/j.surf.2020.100687>
- Das, R.; Ali, M.E.; Hamid, S.B.A.; Ramakrishna, S.; Chowdhury, Z.Z.: Carbon nanotube membranes for water purification: a bright future in water desalination. *Desalination* **336**, 97–109 (2014). <https://doi.org/10.1016/j.desal.2013.12.026>
- Nguyen, D.T.C.; Tran, T.V.; Kumar, P.S.; Din, A.T.M.; Jalil, A.A.; Vo, D.-V.N.: Invasive plants as biosorbents for environmental remediation: a review. *Environ. Chem. Lett.* **20**, 1421–1451 (2022). <https://doi.org/10.1007/s10311-021-01377-7>
- Islam, M.A.; Angove, M.J.; Morton, D.W.; Pramanik, B.K.; Awual, M.R.: A mechanistic approach of chromium (VI) adsorption onto manganese oxides and boehmite. *J. Environ. Chem. Eng.* (2020). <https://doi.org/10.1016/j.jece.2019.103515>
- Kubra, K.T.; Salman, M.S.; Hasan, M.N.; Islam, A.; Teo, S.H.; Hasan, M.M.; Sheikh, M.C.; Awual, M.R.: Sustainable detection and capturing of cerium(III) using ligand embedded solid-state conjugate adsorbent. *J. Mol. Liq.* (2021). <https://doi.org/10.1016/j.molliq.2021.116667>
- Chowdhury, A.K.; Sarkar, A.D.; Bandyopadhyay, A.: Rice husk ash as a low cost adsorbent for the removal of methylene blue and congo red in aqueous phases. *CLEAN—Soil, Air, Water.* **37**, 581–591 (2009). <https://doi.org/10.1002/clen.200900051>
- Saeed, A.; Sharif, M.; Iqbal, M.: Application potential of grapefruit peel as dye sorbent: kinetics, equilibrium and mechanism of crystal violet adsorption. *J. Hazard. Mater.* **179**, 564–572 (2010). <https://doi.org/10.1016/j.jhazmat.2010.03.041>
- Kumar, R.; Ahmad, R.: Biosorption of hazardous crystal violet dye from aqueous solution onto treated ginger waste (TGW). *Desalination* **265**, 112–118 (2011). <https://doi.org/10.1016/j.desal.2010.07.040>
- Kannan, C.; Buvanewari, N.; Palvannan, T.: Removal of plant poisoning dyes by adsorption on tomato plant root and green carbon from aqueous solution and its recovery. *Desalination* **249**, 1132–1138 (2009). <https://doi.org/10.1016/j.desal.2009.06.042>
- Alshabanat, M.; Alsenani, G.; Almufarj, R.: Removal of crystal violet dye from aqueous solutions onto date palm fiber by adsorption technique. *J. Chem.* **2013**, 1–6 (2013). <https://doi.org/10.1155/2013/210239>
- Lin, D.; Wu, F.; Hu, Y.; Zhang, T.; Liu, C.; Hu, Q.; Hu, Y.; Xue, Z.; Han, H.; Ko, T.-H.: Adsorption of dye by waste black tea powder: parameters, kinetic, equilibrium, and thermodynamic studies. *J. Chem.* **2020**, 5431046 (2020). <https://doi.org/10.1155/2020/5431046>
- Nguyen, D.T.C.; Tran, T.V.; Nguyen, T.T.T.; Nguyen, D.H.; Alhasan, M.; Lee, T.: New frontiers of invasive plants for biosynthesis of nanoparticles towards biomedical applications: a review. *Sci. Total Environ.* (2022). <https://doi.org/10.1016/j.scitotenv.2022.159278>
- Panda, S.K.; Aggarwal, I.; Kumar, H.; Prasad, L.; Kumar, A.; Sharma, A.; Vo, D.-V.N.; Van Thuan, D.; Mishra, V.: Magnetite nanoparticles as sorbents for dye removal: a review. *Environ. Chem. Lett.* **19**, 2487–2525 (2021). <https://doi.org/10.1007/s10311-020-01173-9>
- Madikizela, L.M.: Removal of organic pollutants in water using water hyacinth (*Eichhornia crassipes*). *J. Environ. Manage.* **295**, 113153 (2021). <https://doi.org/10.1016/j.jenvman.2021.113153>
- Jawed, A.; Kar, P.; Verma, R.; Shukla, K.; Hemanth, P.; Thakur, V.K.; Pandey, L.M.; Gupta, R.K.: Integration of biological control with engineered heterojunction nano-photocatalysts for sustainable and effective management of water hyacinth weed. *J. Environ. Chem. Eng.* **10**, 106976 (2022). <https://doi.org/10.1016/j.jece.2021.106976>
- Gaurav, G.K.; Mehmood, T.; Cheng, L.; Klemeš, J.J.; Shrivastava, D.K.: Water hyacinth as a biomass: a review. *J. Clean. Prod.* **277**, 122214 (2020). <https://doi.org/10.1016/j.jclepro.2020.122214>
- Selvam, K.; Govarthanam, M.; Kamala-Kannan, S.; Govindharaju, M.; Senthilkumar, B.; Selvankumar, T.; Sengottaiyan, A.: Process optimization of cellulase production from alkali-treated coffee pulp and pineapple waste using *Acinetobacter* sp. TSK-MASC. *RSC Adv.* **4**, 13045–13051 (2014). <https://doi.org/10.1039/C4RA00066H>
- Sun, X.; Abbass, R.; Ghorqi, M.; Patra, I.; Dwijendra, N.K.A.; Uktamov, K.F.; Jasem, H.: Optimization of dyes and toxic metals removal from environmental water samples by clinoptilolite zeolite using response surface methodology approach. *Sci. Rep.* **12**, 13218 (2022). <https://doi.org/10.1038/s41598-022-17636-8>
- Eddebbagh, M.; Abourriche, A.; Berrada, M.; Zina, M. Ben.; Bennamara, A.: Adsorbent material from pomegranate (*Punica granatum*) leaves: optimization on removal of methylene blue



- using response surface methodology. *J. Mater. Environ. Sci.* **7**, 2021–2033 (2016)
22. Moughaoui, F.; Ouaket, A.; Laaraïbi, A.; Hamdouch, S.; Anbaoui, Z.; Abourriche, A.; Berrada, M.: A novel approach for producing low cost and highly efficient activated carbon for removing cationic dyes. *Mediterr. J. Chem.* **8**, 74–83 (2019)
 23. Karri, R.R.; Tanzifi, M.; Tavakkoli Yarak, M.; Sahu, J.N.: Optimization and modeling of methyl orange adsorption onto polyaniline nano-adsorbent through response surface methodology and differential evolution embedded neural network. *J. Environ. Manage.* **223**, 517–529 (2018). <https://doi.org/10.1016/j.jenvman.2018.06.027>
 24. Tran, T.V.; Nguyen, D.T.C.; Nguyen, T.T.; Pham, Q.T.; Vo, D.-V.N.; Nguyen, T.-D.; Van Pham, T.; Nguyen, T.D.: Linearized and nonlinearized modellings for comparative uptake assessment of metal-organic framework-derived nanocomposite towards sulfonamide antibiotics. *Environ. Sci. Pollut. Res.* (2020). <https://doi.org/10.1007/s11356-020-09312-z>
 25. Saha, P.D.; Chakraborty, S.; Chowdhury, S.: Batch and continuous (fixed-bed column) biosorption of crystal violet by *Artocarpus heterophyllus* (jackfruit) leaf powder. *Colloids Surfaces B Biointerf.* **92**, 262–270 (2012). <https://doi.org/10.1016/j.colsurfb.2011.11.057>
 26. Alp Arici, T.: Highly reusable plant-based biosorbent for the selective methylene blue biosorption from dye mixture in aqueous media. *Int. J. Environ. Sci. Technol.* **19**, 1849–1860 (2022). <https://doi.org/10.1007/s13762-021-03238-w>
 27. Ammar, C.; El-Ghoul, Y.; Jabli, M.: Characterization and valuable use of *Calotropis gigantea* seedpods as a biosorbent of methylene blue. *Int. J. Phytoremediation.* **23**, 1085–1094 (2021). <https://doi.org/10.1080/15226514.2021.1876629>
 28. Uddin, M.K.; Baig, U.: Synthesis of Co_3O_4 nanoparticles and their performance towards methyl orange dye removal: characterisation, adsorption and response surface methodology. *J. Clean. Prod.* **211**, 1141–1153 (2019)
 29. Naderi, P.; Shirani, M.; Semnani, A.; Goli, A.: Efficient removal of crystal violet from aqueous solutions with centaurea stem as a novel biodegradable bioadsorbent using response surface methodology and simulated annealing: kinetic, isotherm and thermodynamic studies. *Ecotoxicol. Environ. Saf.* **163**, 372–381 (2018). <https://doi.org/10.1016/j.ecoenv.2018.07.091>
 30. Bezerra, M.A.; Santelli, R.E.; Oliveira, E.P.; Villar, L.S.; Escalera, L.A.: Response surface methodology (RSM) as a tool for optimization in analytical chemistry. *Talanta* **76**, 965–977 (2008)
 31. Li, H.; Li, Y.; Xiang, L.; Huang, Q.; Qiu, J.; Zhang, H.; Sivaiah, M.V.; Baron, F.; Barrault, J.; Petit, S.; Valange, S.: Heterogeneous photo-Fenton decolorization of orange II over Al-pillared Fe-smectite: response surface approach, degradation pathway, and toxicity evaluation. *J. Hazard. Mater.* **287**, 32–41 (2015). <https://doi.org/10.1016/j.jhazmat.2015.01.023>
 32. Prakash Maran, J.; Manikandan, S.: Response surface modeling and optimization of process parameters for aqueous extraction of pigments from prickly pear (*Opuntia ficus-indica*) fruit. *Dye. Pigment.* **95**, 465–472 (2012). <https://doi.org/10.1016/j.dyepig.2012.06.007>
 33. Mittal, A.; Mittal, J.; Malviya, A.; Kaur, D.; Gupta, V.K.: Adsorption of hazardous dye crystal violet from wastewater by waste materials. *J. Colloid Interface Sci.* **343**, 463–473 (2010). <https://doi.org/10.1016/j.jcis.2009.11.060>
 34. Ghorbani, F.; Younesi, H.; Ghasempouri, S.M.; Zinatizadeh, A.A.; Amini, M.; Daneshi, A.: Application of response surface methodology for optimization of cadmium biosorption in an aqueous solution by *Saccharomyces cerevisiae*. *Chem. Eng. J.* **145**, 267–275 (2008). <https://doi.org/10.1016/j.cej.2008.04.028>
 35. Shirani, M.; Semnani, A.; Haddadi, H.; Habibollahi, S.: Optimization of simultaneous removal of methylene blue, crystal violet, and fuchsine from aqueous solutions by magnetic NaY zeolite composite. *Water, Air, Soil Pollut.* **225**, 2054 (2014). <https://doi.org/10.1007/s11270-014-2054-2>
 36. Neupane, S.; Ramesh, S.T.; Gandhimathi, R.; Nidheesh, P.V.: Pineapple leaf (*Ananas comosus*) powder as a biosorbent for the removal of crystal violet from aqueous solution. *Desalin. Water Treat.* **54**, 2041–2054 (2015). <https://doi.org/10.1080/19443994.2014.903867>
 37. Chakraborty, S.; Chowdhury, S.; Saha, P.: Das: Insight into biosorption equilibrium, kinetics and thermodynamics of crystal violet onto *Ananas comosus* (pineapple) leaf powder. *Appl. Water Sci.* **2**, 135–141 (2012). <https://doi.org/10.1007/s13201-012-0030-9>
 38. Lim, L.B.L.; Priyantha, N.; Mansor, N.H.M.: *Artocarpus altilis* (breadfruit) skin as a potential low-cost biosorbent for the removal of crystal violet dye: equilibrium, thermodynamics and kinetics studies. *Environ. Earth Sci.* **73**, 3239–3247 (2015). <https://doi.org/10.1007/s12665-014-3616-8>
 39. Grassi, P.; Drumm, F.C.; Georgin, J.; Franco, D.S.P.; Dotto, G.L.; Foletto, E.L.; Jahn, S.L.: Application of *Cordia trichotoma* sawdust as an effective biosorbent for removal of crystal violet from aqueous solution in batch system and fixed-bed column. *Environ. Sci. Pollut. Res.* **28**, 6771–6783 (2021). <https://doi.org/10.1007/s11356-020-11005-6>
 40. Putri, K.N.A.; Keereerak, A.; Chinpa, W.: Novel cellulose-based biosorbent from lemongrass leaf combined with cellulose acetate for adsorption of crystal violet. *Int. J. Biol. Macromol.* **156**, 762–772 (2020). <https://doi.org/10.1016/j.ijbiomac.2020.04.100>
 41. Ghazali, A.; Shirani, M.; Semnani, A.; Zare-Shahabadi, V.; Nekoeinia, M.: Optimization of crystal violet adsorption onto date palm leaves as a potent biosorbent from aqueous solutions using response surface methodology and ant colony. *J. Environ. Chem. Eng.* **6**, 3942–3950 (2018). <https://doi.org/10.1016/j.jece.2018.05.043>
 42. Essekre, A.; Aarab, N.; Hsini, A.; Ajmal, Z.; Laabd, M.; El Ouardi, M.; Ait Addi, A.; Lakhmiri, R.; Albourine, A.: Enhanced adsorptive removal of crystal violet dye from aqueous media using citric acid modified red-seaweed: experimental study combined with RSM process optimization. *J. Dispers. Sci. Technol.* **43**, 1359–1372 (2022). <https://doi.org/10.1080/01932691.2020.1857263>
 43. Takabi, A.S.; Shirani, M.; Semnani, A.: Apple stem as a high performance cellulose based biosorbent for low cost and eco-friendly adsorption of crystal violet from aqueous solutions using experimental design: mechanism, kinetic and thermodynamics. *Environ. Technol. Innov.* **24**, 1010947 (2021). <https://doi.org/10.1016/j.eti.2021.101947>
 44. Shakoor, S.; Nasar, A.: Utilization of *cucumis sativus* peel as an eco-friendly biosorbent for the confiscation of crystal violet dye from artificially contaminated wastewater. *Anal. Chem. Lett.* **9**, 1–19 (2019). <https://doi.org/10.1080/22297928.2019.1588162>
 45. Rehman, R.; Majeed, S.: Biosorptive removal of crystal violet dye from aqueous solutions by *ficus religiosa* leaves and *daucus carota* pomace in ecofriendly way. *Int. J. Phytoremed.* **24**, 1004–1013 (2022). <https://doi.org/10.1080/15226514.2021.1991269>
 46. Asghari, E.; Saraji, M.: Evaluating cottonwood seeds as a low-cost biosorbent for crystal violet removal from aqueous matrices. *Int. J. Phytoremed.* (2022). <https://doi.org/10.1080/15226514.2022.2064816>
 47. Pavan, F.A.; Camacho, E.S.; Lima, E.C.; Dotto, G.L.; Branco, V.T.A.; Dias, S.L.P.: Formosa papaya seed powder (FPSP): preparation, characterization and application as an alternative adsorbent for the removal of crystal violet from aqueous phase. *J. Environ. Chem. Eng.* **2**, 230–238 (2014). <https://doi.org/10.1016/j.jece.2013.12.017>



48. Homagai, P.L.; Poudel, R.; Poudel, S.; Bhattarai, A.: Adsorption and removal of crystal violet dye from aqueous solution by modified rice husk. *Heliyon* (2022). <https://doi.org/10.1016/j.heliyon.2022.e09261>
49. Cheruiyot, G.K.; Wanyonyi, W.C.; Kiplimo, J.J.; Maina, E.N.: Adsorption of toxic crystal violet dye using coffee husks: equilibrium, kinetics and thermodynamics study. *Sci. African* **5**, e00116 (2019). <https://doi.org/10.1016/j.sciaf.2019.e00116>
50. Gemici, B.T.; Ucun Ozel, H.; Ozel, H.B.: Adsorption behaviors of crystal violet from aqueous solution using Anatolian black pine (*Pinus nigra* Arnold.): kinetic and equilibrium studies. *Sep. Sci. Technol.* **55**, 406–414 (2020). <https://doi.org/10.1080/01496395.2019.1577268>
51. Tran, T.V.; Nguyen, D.T.C.; Nguyen, T.T.T.; Nguyen, D.H.; Alhasan, M.; Jalil, A.A.; Nabgan, W.; Lee, T.: A critical review on pineapple (*Ananas comosus*) wastes for water treatment, challenges and future prospects towards circular economy. *Sci. Total Environ.* (2022). <https://doi.org/10.1016/j.scitotenv.2022.158817>

Springer Nature or its licensor (e.g. a society or other partner) holds exclusive rights to this article under a publishing agreement with the author(s) or other rightsholder(s); author self-archiving of the accepted manuscript version of this article is solely governed by the terms of such publishing agreement and applicable law.